Heliyon 9 (2023) e12378

Contents lists available at ScienceDirect

Heliyon

journal homepage: www.cell.com/heliyon

Research article

Construction of a metabolism-related gene prognostic model to predict survival of pancreatic cancer patients

Huimin Huang [a,b,1], Shipeng Zhou [b,1], Xingling Zhao [b,1], Shitong Wang [b], Huajun Yu [c,*], Linhua Lan [b,**], Liyi Li [d,***]

[a] School of Laboratory Medicine and Life Sciences, Wenzhou Medical University, University Town, Chashan District, Wenzhou, Zhejiang Province, 325000, PR China
[b] Key Laboratory of Diagnosis and Treatment of Severe Hepato-Pancreatic Diseases of Zhejiang Province, The First Affiliated Hospital of Wenzhou Medical University, Fanhai West Road, Wenzhou, Zhejiang Province, 325000, PR China
[c] Department of Hepatobiliary Surgery, The First Affiliated Hospital of Wenzhou Medical University, Fanhai West Road, Wenzhou, Zhejiang Province, 325000, PR China
[d] The general surgery department of second affiliated hospital of Wenzhou medical university, No. 109, College West Road, Wenzhou, Zhejiang Province, 325002, Zhejiang, PR China

ARTICLE INFO

Keywords:
Metabolism-related genes
Immune-related genes
Pancreatic cancer
Prognostic model

ABSTRACT

Pancreatic cancer (PC) is one of the most fatal malignant tumors, and is commonly diagnosed at an advanced stage with no effective therapy. Metabolism-related genes (MRGs) and immune-related genes (IRGs) play considerable roles in the tumor microenvironment. Therefore, an effective prediction model based on MRGs and IRGs could aid in the prognosis of PC. In this study, differential expression analysis was performed to gain 25 intersectional genes from 857 differentially expressed MRGs (DEMRGs), and 1353 differentially expressed IRGs, from The Cancer Genome Atlas database of PC. Cox and Lasso regression were applied and a five-DEMRGs prognostic model constructed. Survival analysis, ROC values, risk curve and validation analysis showed that the model could independently predict PC prognosis. In addition, the correlation analysis suggested that the five-DEMRGs prognostic model could reflect the status of the immune microenvironment, including Tregs, M1 macrophages and Mast cell resting. Therefore, our study provides new underlying predictive biomarkers and associated immunotherapy targets.

1. Introduction

Pancreatic cancer (PC) is one of the most lethal tumors, and is set to become the second deadliest malignancy in the USA by 2025 [1]. Currently, surgery is the only method to potentially cure PC. However, only up to 20% of patients have a chance of initial surgical resection due to the lack of sensitive diagnostic screening analysis for early stage PC. Even for those patients for whom surgery is successful, more than 80% of patients will eventually develop local recurrence or metastasis [2, 3]. Current interventions to prevent, diagnose, and treat PC are insufficient, leading to poor prognosis [4]. To date, models based on clinical and pathological parameters,

* Corresponding author.
** Corresponding author.
*** Corresponding author.
E-mail addresses: yuhuajun@wmu.edu.cn (H. Yu), paullee90@wmu.edu.cn (L. Lan), liliyi@wmu.edu.cn (L. Li).
[1] These authors made equal contributions to this manuscript.

https://doi.org/10.1016/j.heliyon.2022.e12378
Received 17 February 2022; Received in revised form 15 May 2022; Accepted 7 December 2022
Available online 17 December 2022

such as the American Joint Committee on Cancer (AJCC) staging system, have been applied to evaluate prognosis [5]. However, this cannot be dynamically adjusted as the patient's condition changes. Additionally, this system does not reflect the biological behavior of the tumor at the molecular level [6]. Hence it is necessary to develop personalized prediction methods for PC patients.

One of the emerging hallmarks of cancer is reprogrammed cellular energy metabolism [7, 8]. Dysregulated metabolism satisfies the requirements of ideal survival and rapid proliferation of cancer cells[9]. Furthermore, the Warburg effect (anaerobic glycolysis) permits cancer cells to take up glucose and convert pyruvate into lactic acid despite insufficient oxygen [10]. Recent studies have indicated that metabolic alterations can also promote tumorigenesis and metastasis of PC through epigenetic regulation [11, 12]. Therefore, the relationship between metabolism and PC is crucial for understanding the pathogenesis in tumorigenesis. However, few studies have analyzed the correlation of metabolism-related genes (MRG) and the prognosis and survival of PC by high-throughput biomarker sequencing. However, due to the complexity of the tumor microenvironment [13], a single prognostic biomarker may not be sufficient to predict the clinical outcomes of PC.

The overgrowth of the extracellular matrix in PC had been discovered to lead to the formation of barriers against the immune system, drug delivery, oxygen and nutrients. In order to supply nutrients to survive, the cells develop mechanisms that alter the typical metabolic pathways [14]. Through reprogramming and improving the immune response, immunotherapy facilitates anti-tumor activities [15]. Metabolic pathways can either inhibit or promote immune cell functions and the differentiation, and functions of immune cells have enormous impacts with metabolism, hence a combination of the two ways may be a more effective treatment option [16].

A recent study had developed a novel metabolic-related signature to predict the overall survival for PC [17], while another study constructed a prognostic model based on immune-related genes for the prediction of survival in PC [18]. However, there is no prediction model that takes both metabolic and immune genes into account to establish a model. Since the metabolism and immune systems are both the significant hallmarks of cancer, they may take part in the development of PC to a certain extent together. Here, we aimed to identify differentially expressed metabolism-related genes (DEMRGs) and immune-related genes (DEIRGs) in PC. Furthermore, the intersectional genes from DEMRGs and DEIRGs were discovered, and a prognostic prediction model created from systematically analyses of intersectional genes expressions and their association with clinic and prognosis. A series of bioinformatics analyses revealed and validated the potential molecular mechanisms of this prediction model. This study could therefore provide prognostic value for patients and offer a new basis for tumor therapy of PC.

2. Materials and methods

2.1. Acquisition of gene expression and clinical data

RNA sequencing transcriptomics data and clinicopathological characteristics were downloaded from The Cancer Genome Atlas (TCGA) database (https://portal.gdc.cancer.gov), including 4 normal cases and 178 tumor cases. In view of the small scale of the normal cases in TCGA database, we obtain extra 167 mRNA expression data of normal tissue from the Genotype-Tissue Expression (GTEx) cohort in the University Of Cingifornia Sisha Cruz (UCSC) Xena database (https://xenabrowser.net/datapages/). "normalize Between Array" function in R language (version 4.0.2) were applied to combined with the gene expression data from the above two databases. The Perl and the R programming languages and the original data and the converted data were shown in Supplementary **1, 2, 3 and 4. The metabolism-related gene set (Supplementary **5) was downloaded from Molecular Signature Database (MSigDB) using Gene Set Enrichment Analysis tool (GSEA, https://www.gsea-msigdb.org/gsea/index.jsp). While immune related genes were obtained using the ImmPort database (http://www.immport.org/) (Supplementary **5). Besides, the cBioPortal tool (https://www.cbioportal.org) database was carried out to display the alternation characteristics of MRGs.

Furthermore, mRNA expression data of PC were searched and downloaded from the ICGC-PAAD-US from International Cancer Genome Consortium (ICGC) database (https://icgc.org/) as well as the Gene Expression Omnibus (GEO) database (https://www.ncbi.nlm.nih.gov/gds/). GSE28735 dataset from the GEO database using the keywords "pancreatic cancer", "PC", "microarray" and "adjacent". The datasets were selected for the following criteria: (1) human pancreatic tissue samples; (2) $\geq$30 samples; (3) tumor and adjacent non-tumor pancreatic control samples.

2.2. Differential expression analysis

The DEMRGs and DEIRGs in PC were detected using the "limma" package in R language. False discovery rate (FDR) < 0.05 by a Wilcoxon rank-sum test was considered as significant. The "pheatmap" package was run to screen the heat-maps in R language loaded with differentially expression gene files.

2.3. Enrichment analysis

Gene ontology (GO) along with Kyoto Encyclopedia of Genes and Genomes (KEGG) pathway enrichment analyses were selected by the "clusterProfiler", "ggplot2", "org.Hs.eg.db" and "enrichplot" packages. Additionally, p-values less than 0.05 of samples were considered to be significantly enriched.

2.4. Protein–Protein Interaction network construction

The Search Tool for the Search Tool for the Retrieval of Interacting Genes/Proteins (STRING) database could provide the

interaction information of genes/proteins. We utilized this database to construct a Protein-Protein Interaction (PPI) network. Nodes where the interactive relationships were greater than 0.4 were selected to build the network.

2.5. Prognostic-related MRGs

To obtain prognostic-related MRGs in PC, we used the "survival" package in R language to perform the univariate Cox regression analysis ($P < 0.001$). Based on Hazard Ratio (HR), prognostic-related MRGs were categorized into high risk MRGs (HR > 1) and low risk MRGs (HR > 1).

2.6. Construction and validation of the MRGs prognostic model

The least absolute shrinkage and selection operator (Lasso) and multivariate Cox proportional hazard regression analysis were further developed to construct the prediction model with "survival" package in R language. The formula of the prognostic model of PC patients' prognosis was as follows: risk score = the sum of the multivariate Cox regression coefficient variation of each mRNA. Also, "survival" package was employed for receiving the survivorship curve with the survival probability of two groups. Additionally, receiver operating characteristic (ROC) curve along with area under the curve (AUC) value were implemented by the package "survivalROC". AUC values could evaluate the prognostic model to uncover the prognostic biomarkers in PC, with values between 0.5-0.7 representing moderate, 0.7–0.9 standing for better, as well as more than 0.9 describing as superior.

2.7. Independent analysis and correlation analysis of clinical characteristics and five-DEMRGs in prognostic model

Univariate and multivariate independent prognostic analyses, loaded with the "survival" package in R language, were implemented to identify the potential role of MRGs in prognostic model. Based on the Kruskal-Wallis rank-sum test, the "ggpubr" package in R language was applied to explore the relationships between five-DEMRGs and the clinico-pathological parameters. Parameters with $p < 0.05$ were considered statistically significant.

2.8. Gene Set Enrichment Analysis

Served as the target set, C2.cp.kegg.v7.2.symbols.gmt was applied to run Gene Set Enrichment Analysis (GSEA) analysis of all tumor cases with GSEA (version 4.1.0) downloaded from the Broad Institute. Gene sets with NOM p-values < 0.05 were considered as statistically significant.

2.9. Evaluation of tumor infiltrated immune cells in prognostic model

The CIBERSORT algorithm was utilized to calculate the fractions of the tumor infiltrated immune cells of all tumor cases. Data with p-values less than 0.05 were filtered and selected for further analysis with the "limma" package in R language. Difference and correlation analyses were carried out with the "limma", "vioplot", "gglot2", "ggpubr" and "ggExtra" packages. Only p-values less than 0.05 were regarded as statistically significant using the Wilcoxon rank-sum and Pearson coefficient tests.

2.10. Cell lines and cell culture

HPDE, a pancreatic normal ductal epithelial cell line, together with PC cell lines CFPAC-1, BXPC-3, PANC-1 and MIA PaCa-2 were all purchased from the Cell Bank of the Chinese Academy of Science (Shanghai, China). HPDE, PANC-1 and MIA PaCa-2 were cultured in DMEM basal medium while CFPAC-1 and BXPC-1 in RPMI-1640 basal medium (GIBCO, US). Besides, all cell lines were supplemented with 10% fetal bovine serum (GIBCO, US), 1% penicillin and 1% streptomycin (Beyotime, China) in cell incubator at 37 °C, 5% CO_2.

2.11. Protein extraction and Western blot analysis

All cell line samples were collected in microcentrifuge tubes and treated with Triton-X100 lysis buffer for 20 min at 4 °C. Then, the samples were centrifuged at 12500 rpm for 15 min at 4 °C to gain the supernatants. The protein concentrations were determined by BCA protein concentration detection kit and boiled with sample buffer for 5 min at 95 °C. 20 μg of protein samples were separated on 12% SDS-PAGE gels and transferred to 0.22 μm polyvinylidene fluoride (PVDF) membranes. Then, the membranes were blocked in 5% non-fat milk for 1.5 h at room temperature. The membranes were incubated with primary antibody overnight at 4 °C. Next day, the blots were washed with TBST buffer and then incubated for 1 hr with gently rinsing in the HRP-conjugated secondary antibodies solution. Western blots were incubated with ECL substrate for 1 min then visualized using ultra-sensitive multifunctional imager. PIK3CA (A16950, ABclonal), ARG2 (14825-1-AP, Protein technology Group), IDO1 (13268-1-AP, Protein technology Group), PTGS2 (A3560, ABclonal), PLCG1 (A8899, ABclonal) and Actin (ACO26, ABclonal) were purchased and used in this study.

2.12. Statistical analysis

All analyses were accomplished by R language version 4.0.2. Unless otherwise declared, $p < 0.05$ was considered to be significant.

3. Results

3.1. Identification of DEMRGs and DEIRGs

A flowchart of the analysis procedure for this study is summarized in Figure 1. Differential expression analyses identified DEMGRs and DEIRGs. A heat-map indicates how PC cases could be distinguished from normal cases (Figure 2A, B). LogFC > 0 on behalf of the up-regulated genes while logFC < 0 represent the down-regulated genes. A total of 857 DEMRGs (782 up-regulated, and 75 down-regulated) and 1353 DEIRGs (1260 up-regulated & 93 down-regulated) were identified in tumor samples when compared with

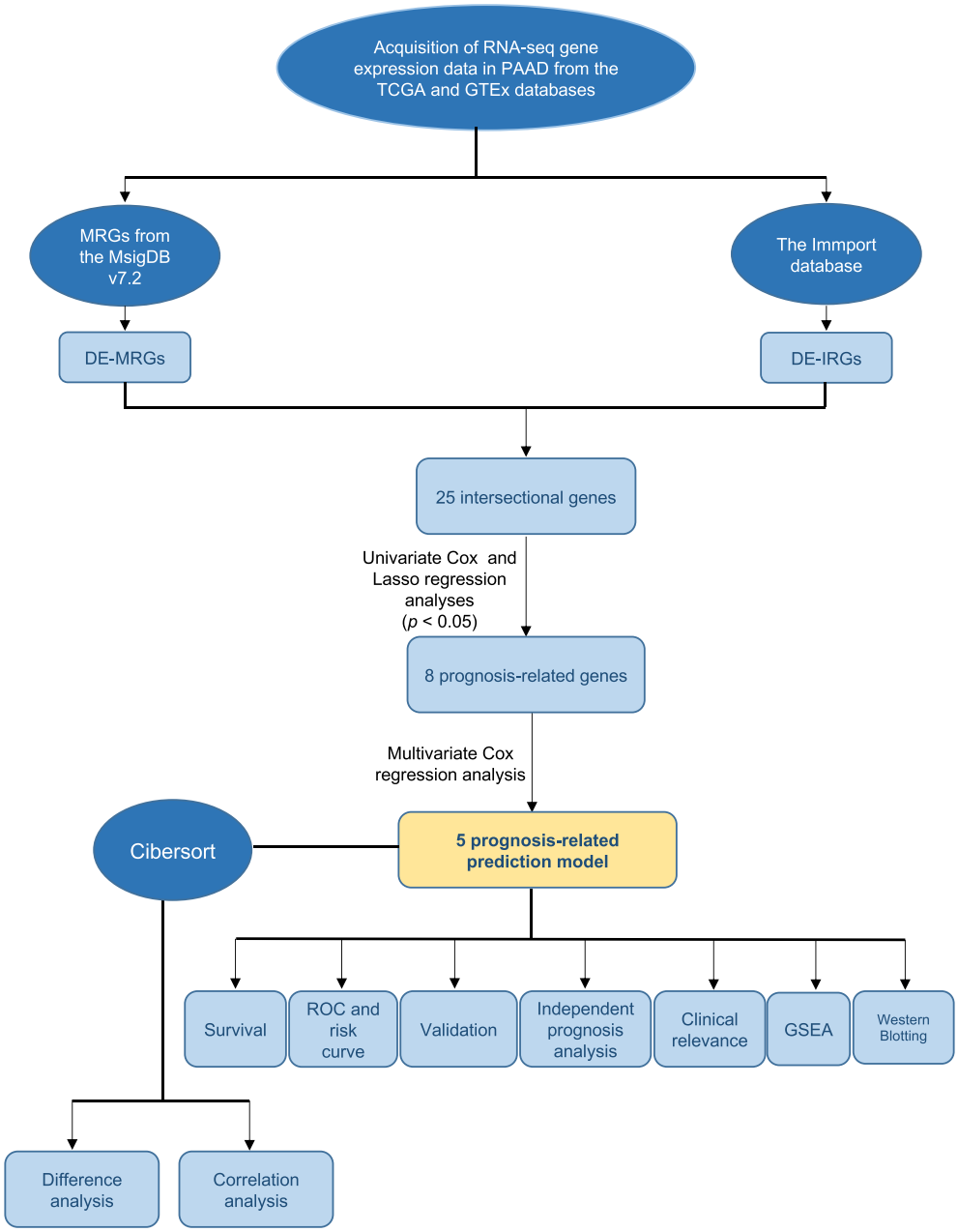

Figure 1. Flowchart of the data analyses procedure.

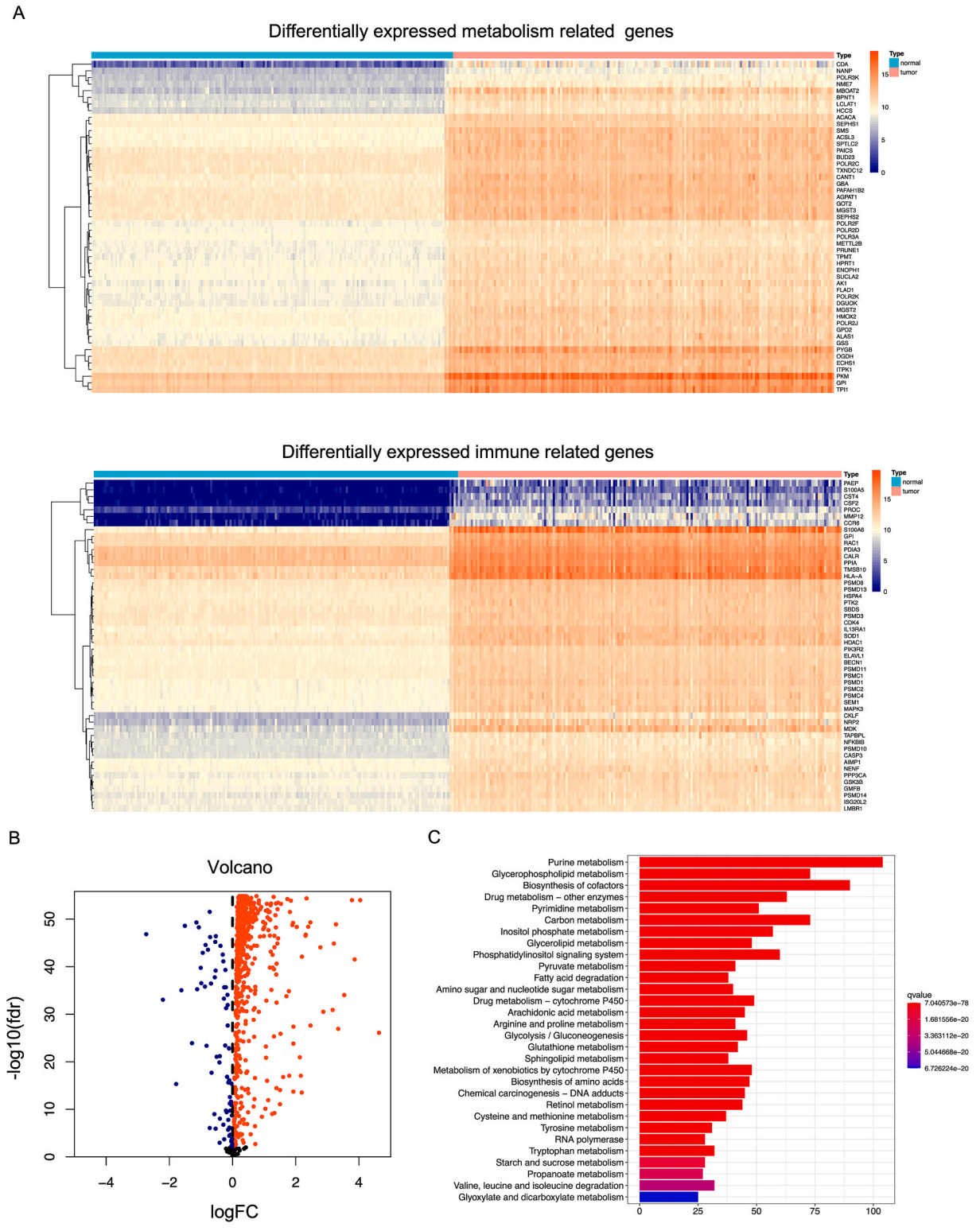

Figure 2. Identification of DEMRGs and DEIRGs. (A, B) Heat-map and volcano of significantly DEMRGs and DEIRGs in PAAD. The color from red to blue represents the progression from high expression to low expression. (C) Top 30 pathway from KEGG enrichment analysis of DEMRGs.

normal samples (Supplementary **6 and 7). The results of KEGG pathway enrichment analysis indicated that these DEMRGs were associated with signaling pathways related to material and synthesis metabolism (Figure 2C).

3.2. Twenty five intersectional genes were discovered from the intersections of DEMRGs and DEIRGs

Intersections between the up-regulated or down-regulated DEMRGs and DEIRGs were visualized in Venn diagrams (Figure 3A). Figure 3B shows 24 common differentially expressed genes that were up-regulated, and one common differentially expressed gene that was down-regulated in both DEMRGs and DEIRGs. In order to visualize potential interactions between these 25 DEMRGs, PPI network construction based on the STRING database was performed that covered 25 nodes and 43 edges (Figure 3C). Therefore, a total of 25 DEMRGs may be crucial in the pathology of PC.

3.3. Construction of the five-DEMRGs prognostic model for PC

To further screen the genes related to the prognosis of PC, univariate Cox and Lasso regression analyses were employed from 25 DEMRGs. And these two analyses screened out eight DEMRGs, which incorporated five high-risk DEMRGs and three low-risk DEMRGs

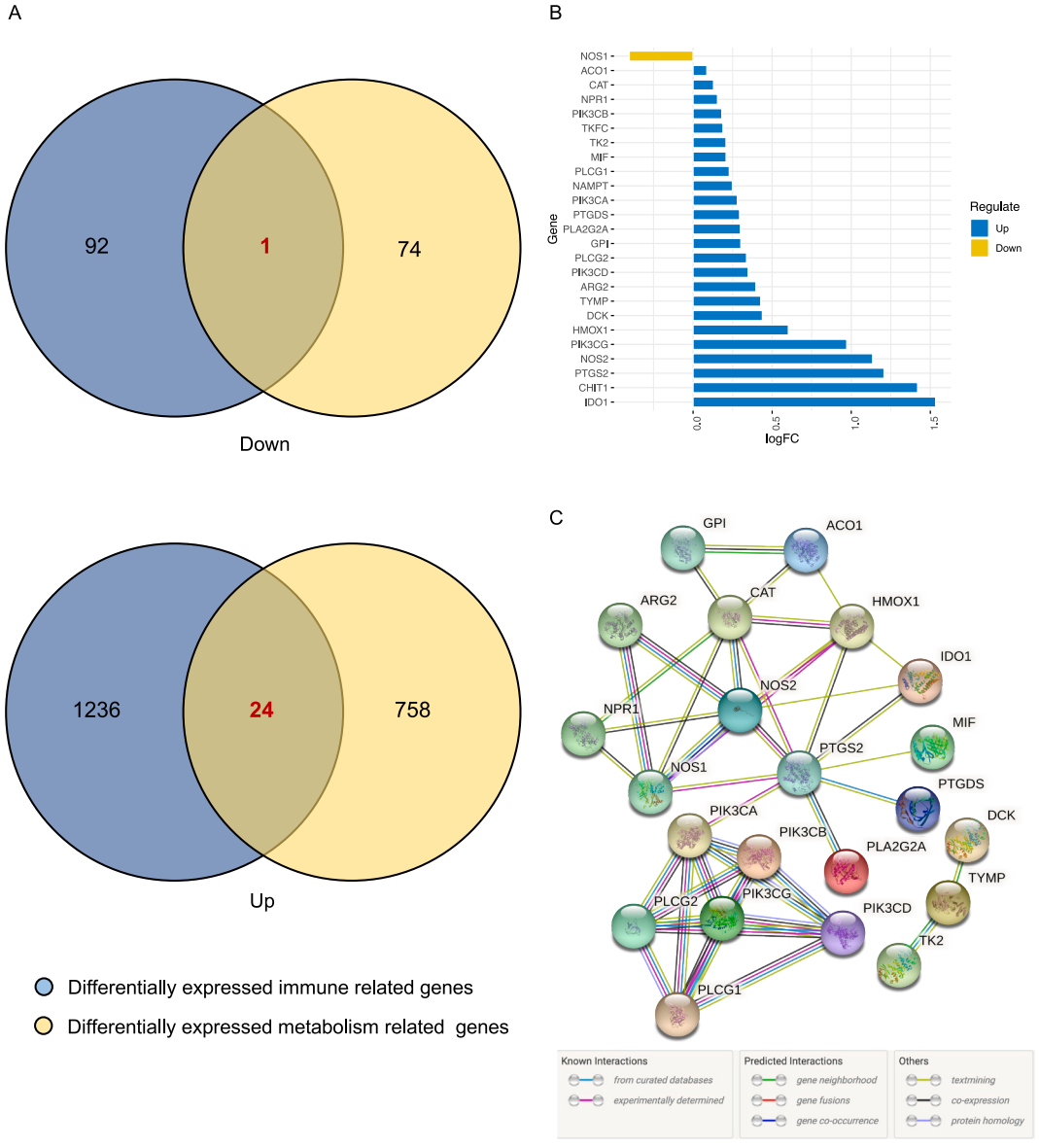

Figure 3. Intersection and PPI network construction of 25 DEMRGs. (A, B) The international genes of up- and down-regulated DEMRGs and DEIRGs. (C) PPI network construction with hiding disconnected nodes.

A

	pvalue	Hazard ratio
PIK3CA	0.005	1.238(1.065–1.439)
IDO1	0.002	1.027(1.009–1.044)
ARG2	0.025	0.774(0.618–0.969)
PTGS2	0.010	1.013(1.003–1.024)
NPR1	0.032	0.870(0.766–0.988)
NAMPT	0.013	1.031(1.006–1.056)
PIK3CB	<0.001	1.242(1.114–1.385)
PLCG1	0.005	0.874(0.796–0.959)

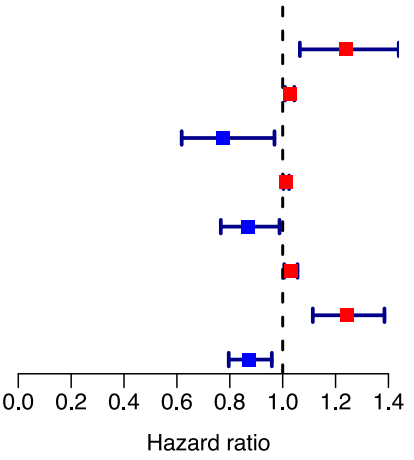

B

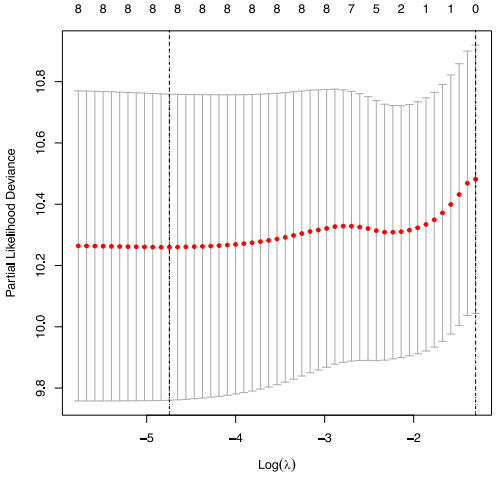

C

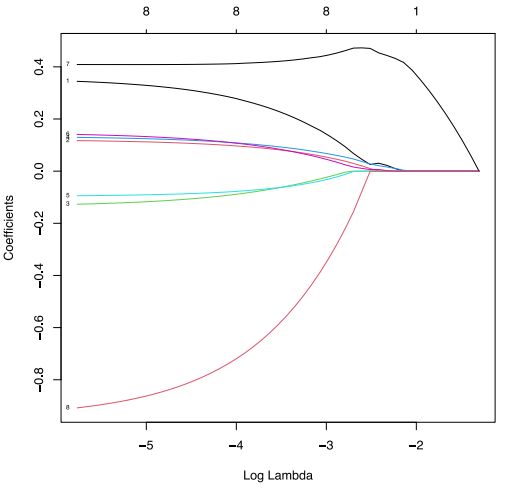

D

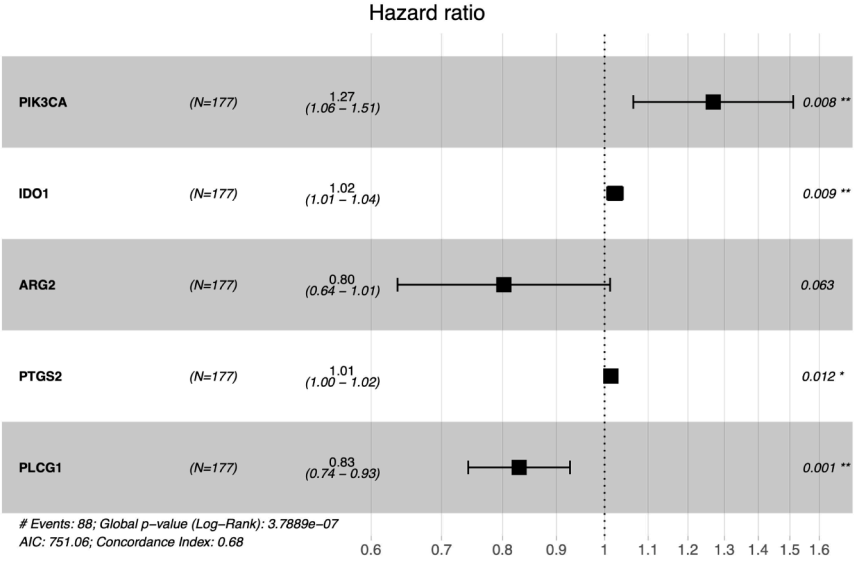

(caption on next page)

Figure 4. Construction of the five-DEMRGs prognostic model with 25 DEMRGs. (A) Univariate Cox regression analysis of 8 DEMRGs. Red and blue dots indicate the high-risk and low-risk respectively. (B) Screening of optimal parameter (λ) at which the vertical lines were drawn. (C) Lasso coefficient profiles of the 8 DEMRGs with non-zero coefficients determined by the optimal λ. (D) Multivariate Cox regression analysis was applied to construct the five-DEMRGs prognostic model.

(Figure 4A, B, C). Additionally, multivariate Cox regression proportional hazard analysis was applied among eight prognostic-related DEMRGs, which found five-DEMRGs could construct the prognostic model to independently predict the prognosis of PC (Figure 4D). Phosphatidylinositol-4,5-bisphosphate 3-kinase Catalytic Subunit Alpha (PIK3CA), Indoleamine 2,3-dioxygenase 1 (IDO1) and Prostaglandin-endoperoxide Synthase 2 (PTGS2) with HR $>$ 1 were considered as oncogenes, whereas Arginase 2 (ARG2) and Phospholipase C Gamma 1 (PLCG1) with HR $<$ 1 were regarded as tumor suppressors (Table 1). The risk scores calculated from the prognostic model were as follows:

Risk score = 0.2378 * PIK3CA expression +0.0228* IDO1 expression + (−0.2205) * ARG2 expression +0.0137 * PTGS2 + (−0.1870) * PLCG1 expression.

Furthermore, we also validated the protein expressions of these five-DEMRGs by western blotting analysis and found that most were highly expressed in PC cell lines (Figure 5).

3.4. General gene expression and alteration characteristics of five-DEMRGs

The mRNA expression levels of five genes were significantly increased in PC samples from our data and GEPIA database (Supplementary *1A and B). Supplementary *1C and D show the top ten GO terms and pathways of the above five genes by GO and KEGG enrichment functional analyses. Furthermore, genomic alterations and potential drugs of the five-DEMRGs were analyzed by the cBioPortal tool. Of the samples 12.1% presented with alterations in the five-DEMRGs, while PIK3CA and IDO1 were the most commonly altered genes; with amplification being the main type of genetic alteration (Supplementary *2).

3.5. Validation of the accuracy of the five-DEMRGs prognostic model

According to the median risk score, all samples were averagely divided into high- and low-risk groups. As survival analysis revealed, high-risk groups in PC were correlated with poorer prognosis compared with low-risk groups ($p < 0.001$; Figure 6A). ROC curve was performed to evaluate the specificity and sensitivity of the five-DEMRGs prognostic model. Additionally, AUC values at years 1, 2, and 3 were 0.755, 0.682 and 0.657, respectively (Figure 6B), indicating that the five-DEMRGs prognostic model showed better accuracy in survival prediction. A heat-map distribution of the five-DEMRGs is shown in Figure 6E. As the risk score increased, the amounts of surviving patients decreased while the number of dead patients increased (Figure 6C). Furthermore, the prognosis of the low-risk group sample is significantly better than that of the high-risk group (Figure 6D).

ICGC-PAAD-US from the ICGC database and GSE28735 dataset from the GEO database were performed to validate the prediction performance of the five-DEMRGs model. Risk scores of all samples were calculated using the same formula. As shown in Figure 6F and G, high-risk groups had markedly worse survival than low-risk groups in other online databases. In addition, we also performed a Lasso regression analysis, a commonly used method in bioinformatics modelling, and found an eight-DEMRGs model of PC. According to the ROC analyses of the five- (based on multivariate Cox regression analysis) and eight-DEMRGs model (on the basis of the Lasso regression analysis), the AUC at 2 or 3 years of the former was more accurate than that of the latter (Figure 6B and Supplementary *5A). As such, these consequences demonstrated that the five-DEMRGs model could indeed accurately predict the prognosis of PC.

3.6. Risk score from the five-DEMRGs prognostic model could be an independent predictor of PC

Independent prognosis analysis was carried out to further verify the correlation of risk scores and PC prognosis. The hazard ratio of the risk score was 1.188 (1.115–1.267) with $p < 0.001$ from univariate independent prognostic analysis (Figure 7A), while multivariate independent prognostic analysis revealed a hazard ratio of the risk score of 1.173 (1.097–1.255) with $p < 0.001$ (Figure 7B). The higher the risk score, the poorer the prognosis. These data were clinically and statistically significant, which indicated risk scores could be independent predictors of PC. Combined with age, gender, histological grade and stage, the five-DEMRGs prognostic risk score was applied to draw a ROC survival curve. Compared to other clinical characteristics, the five-DEMRGs prognostic risk scoring model was more accurate at predicting the 1, 2, and 3 year survival rate of PC samples (Figure 7C, AUC = 0.742, 0.657 and 0.611, respectively).

Table 1
Multivariate Cox regression analysis.

ID	coef	HR	HR.95L	HR.95H	p-values
PIK3CA	0.2378	1.2685	1.0649	1.5110	0.008
IDO1	0.0228	1.0231	1.0057	1.0408	0.009
ARG2	−0.2205	0.8021	0.6357	1.0121	0.063
PTGS2	0.0137	1.0138	1.0031	1.0247	0.012
PLCG1	−0.1870	0.8295	0.7420	0.9272	0.001

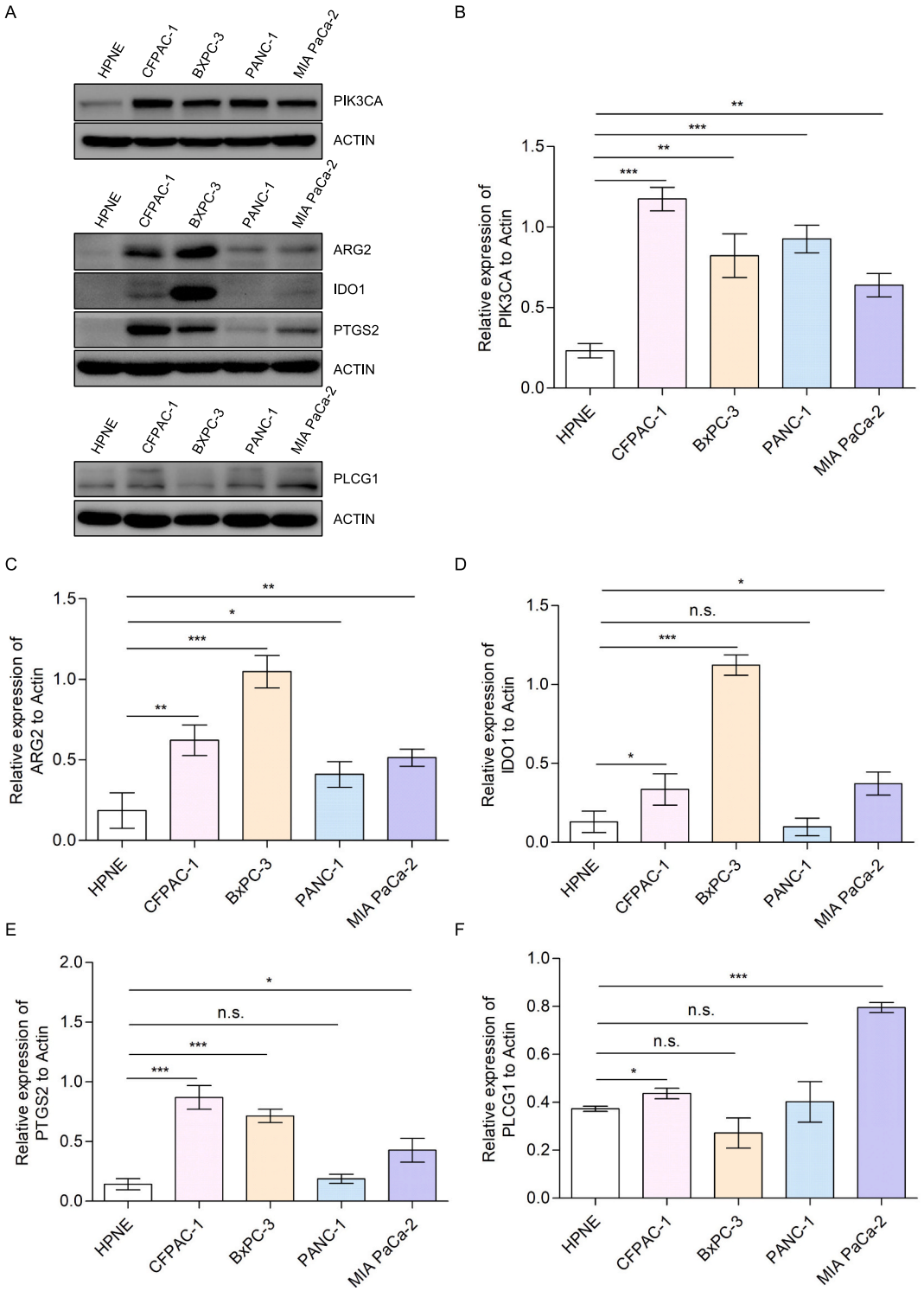

Figure 5. The protein expressions of the five-DEMRGs in pancreatic cancer and normal cell lines. **(A)** The level of five genes were tested by western bolt analysis with antibodies against indicated molecules in HPNE, CFPAC-1, BXPC-3, PANC-1 and MIA PaCa-2 cell lines. **(B–F)** Quantitative analysis of the protein expression of the five-DEMRGs in pancreatic cancer and normal cell lines. Data are shown as Mean ± SD. n.s. no significance, *p < 0.05, **p < 0.01, ***p < 0.001.

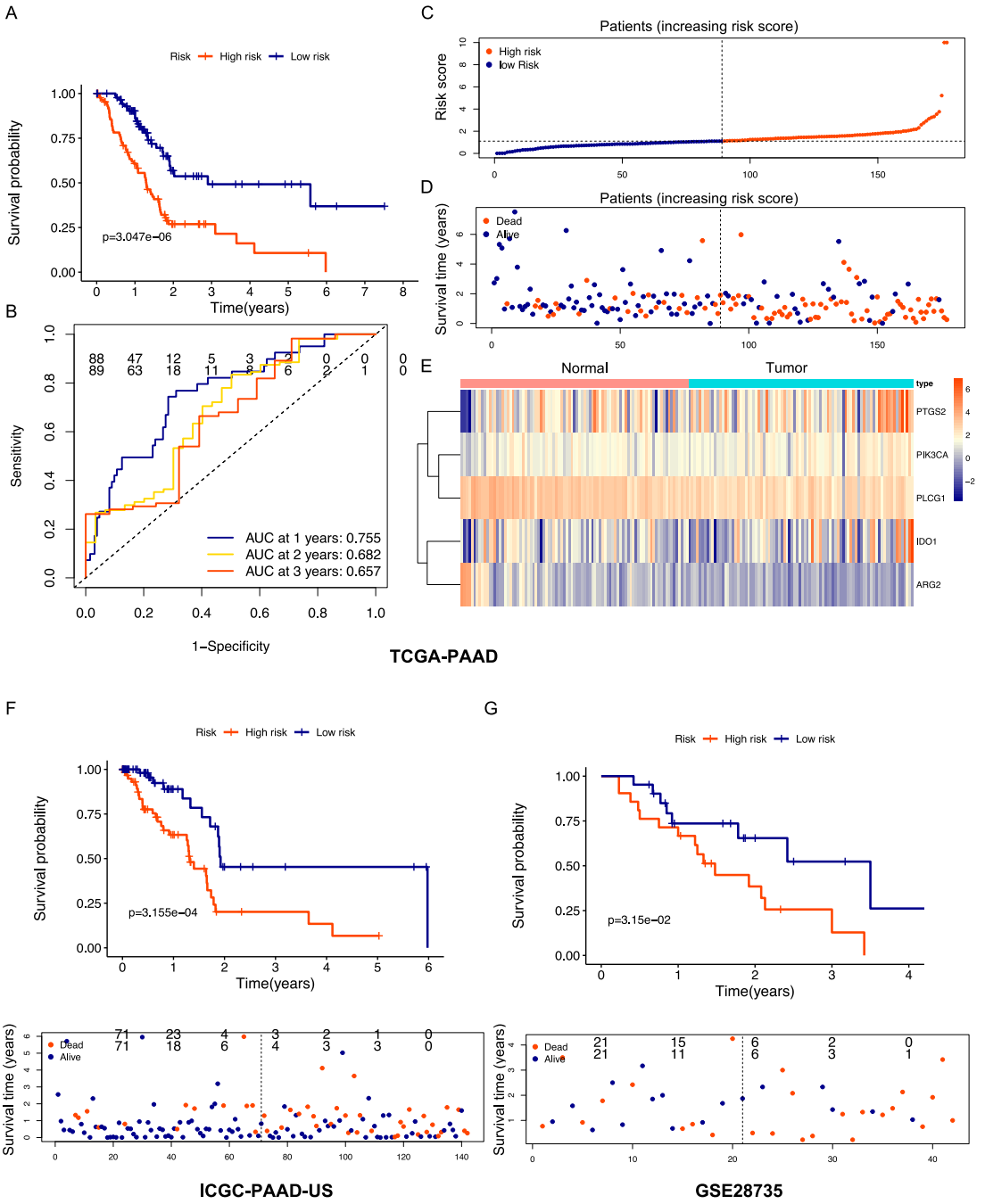

Figure 6. Validation of the accuracy of the five-DEMRGs prognostic model. **(A)** The accuracy of prognostic model in TCGC database. OS curve for patients in high-risk group (red curve) and low-risk group (blue curve). (B) ROC curve analysis for the feasibility of five-DEMRGs prognostic model. (C–E) The risk score, survival status and a risk heat-map analyses for patients of high-risk group and low-risk group. (F and G) The accuracy of prognostic model in the ICGC and GEO databases.

3.7. Five-DEMRGs are strongly correlated with prognosis and the clinico-pathological characteristics of PC patients

The clinico-pathological statistics of PC patients in the TCGA database are listed in Table 2. Furthermore, the Wilcoxon rank-sum test was carried out and showed the correlation of five-DEMRGs and clinico-pathological characteristics (Supplementary **8). The heat-map presents the expression levels of the five-DEMRGs in high-risk and low-risk groups with clinical characteristics (Supplementary *3A). As shown in Supplementary *3B, PIK3CA, ARG2 and PTGS2 expression levels were significantly associated with age, histological grade, stage and T classification respectively. Furthermore, Supplementary *4 displayed the correlation of

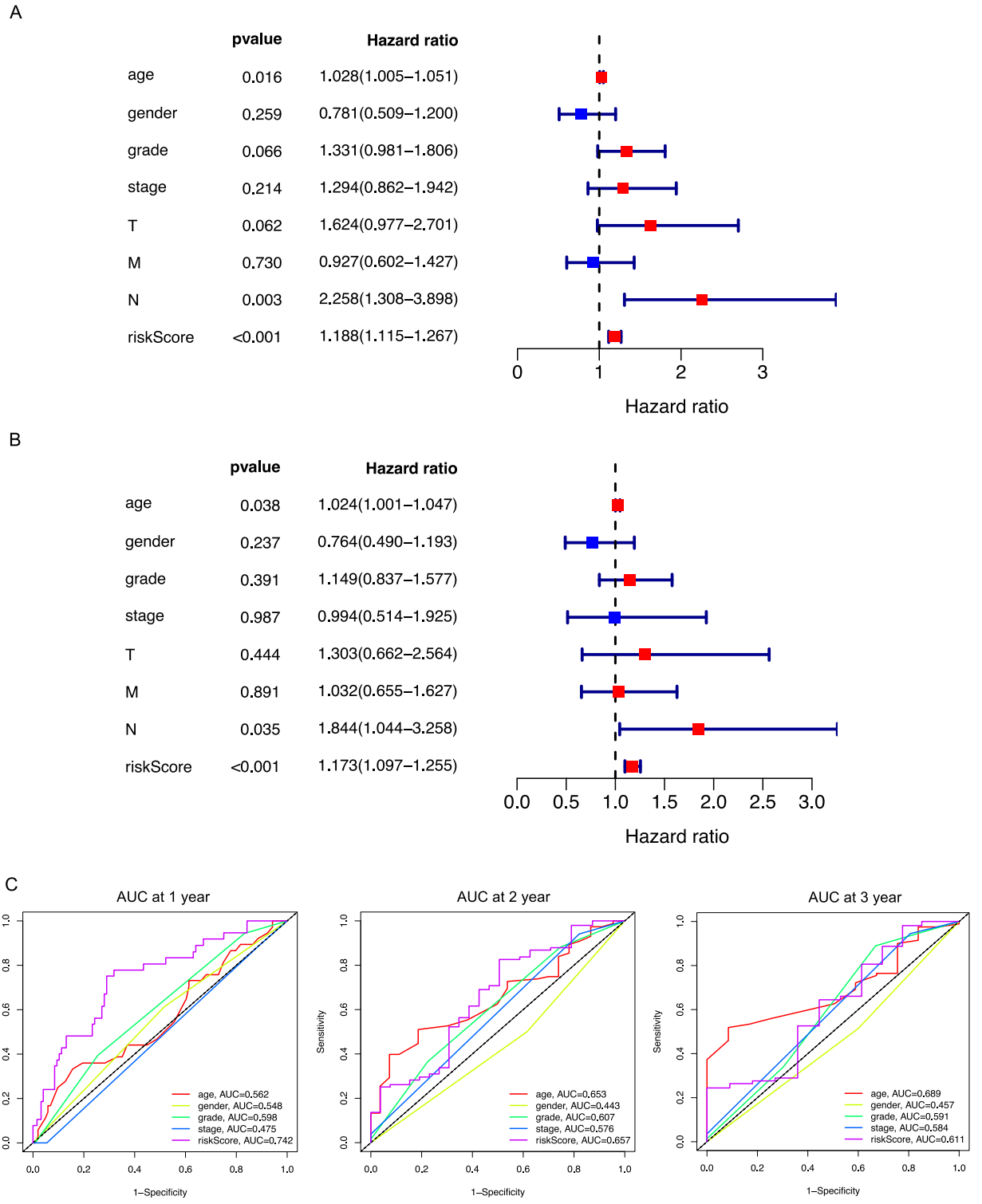

Figure 7. Independent prognostic analyses and ROC curve of risk scores and clinical characteristics. (A) Forest plots of univariate independent prognostic analysis. (B) Forest plots of multivariate independent prognostic analysis. (C) ROC curve of 1-, 2-, and 3-year OS for multiple prognostic indicators of PPAD samples.

Table 2
Clinico-pathological characteristics statistics of PAAD patients.

Clinical characteristics		Mean ± SD	Percentages
Follow-up time		584.36 ± 464.72	
Survival status	Alive	81	49.09%
	Dead	84	50.91%
Age	≤65	79	47.88%
	>65	86	52.12%
Gender	Male	90	54.55%
	Female	75	45.45%
Grade	G1	27	16.36%
	G2	90	54.55%
	G3	44	26.67%
	G4	2	1.21%
	Not available	2	1.21%
Stage	I	19	11.52%
	II	137	83.03%
	III	2	1.21%
	IV	4	2.42%
	Not available	3	1.82%
T	T1	7	4.24%
	T2	21	12.73%
	T3	133	80.61%
	T4	2	1.21%
	Not available	2	1.21%
M	M0	73	44.24%
	M1	4	2.42%
	Mx	88	53.33%
N	N0	47	28.48%
	N1	113	68.48%
	Not available	5	3.03%

clinicopathological factors and prognosis., and we found T classification and N classification could affect the prognosis in PC. These data suggested that the five-DEMRGs were closely related to the clinical progression of PC.

3.8. Gene Set Enrichment Analysis

To further confirm the association of risk scores and the metabolism pathway, the C2 Kegg collection from MSigDB in GSEA was used to analyze data between the high- and low-risk groups. The high-risk group was enriched in starch and sucrose metabolism whilst the low-risk group was enriched in ABC transporters, the calcium signaling pathway, glycosaminoglycan biosynthesis chondroitin sulfate, glycosphingolipid biosynthesis ganglio series, GNRH signaling pathway, long term depression, MTOR signaling pathway, neuroactive ligand receptor interaction, and taste transduction (Figure 8A, B and Table 3).

3.9. Risk scores impact the immune activity of the tumor microenvironment

In order to explore the association between risk scores and the immune microenvironment, fractions of tumor infiltrated immune cells were analyzed via CIBERSORT. Figure 9A, B display the difference and correlation of tumor infiltrated immune cells. Through the intersection of these above two analyses, two kinds of tumor infiltrating immune cells were positively associated with risk scores, which included M1 macrophages and Mast cells resting. Regulatory T cells (Tregs) were shown to be negatively correlated with risk scores (Table 4).

3.10. Risk scores are closely correlated with immune checkpoint genes

Immune checkpoint genes (ICGs) play vital roles in circumventing self-reactivity and may be novel cancer targets [19]. The expression of 79 ICGs of PC (Supplementary ** 9), identified from the literatures [20, 21, 22], were downloaded from the TCGA database. We clustered the PC samples into different groups using the "ConsensusClusterPlus" package on the basis of the expression of the ICGs. There was the lowest crossover between the PC samples when the consensus matrix k value was equal to 3, which divided the PC patients cohort into three clusters, namely clusters 1, 2 and 3 (Supplementary *5B–D). According to a Kaplan-Meier survival analysis for the clustered samples, the survival curve revealed significantly better overall survival in cluster 3 compared with other clusters (Supplementary *5E), suggesting that the ICGs could classify the PC samples at a prognostic level. Furthermore, we also carried out a differential analysis of the ICGs between high- and low-risk groups (Supplementary *6). The ICGs listed in Supplementary ** 10, show a significant correlation between high- and low-risk groups.

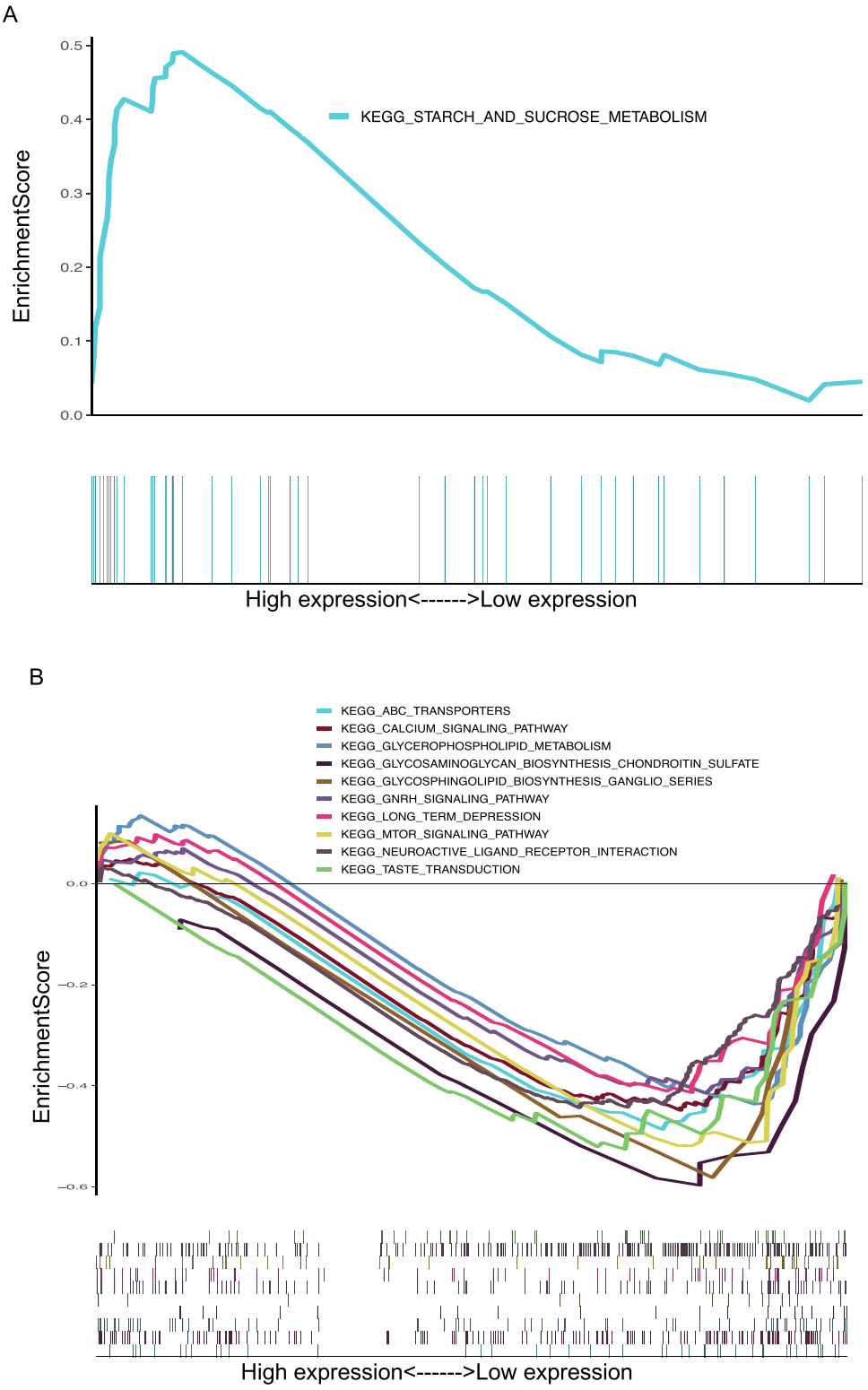

Figure 8. GSEA analysis of risk score of prognostic model in PAAD. (A) The enriched gene sets in C2 kegg collection by the high-risk group. (B) The enriched gene sets in C2 kegg collection by the low-risk group. Each color represented corresponding gene set. Genes on the right of X-axis had positive correlation with gene sets, while genes on the left of X-axis had negative correlation with gene sets. Only gene sets with NOM p value <0.05 were considered as statistically significant.

Table 3
Enriched gene sets.

C2 kegg collection	Gene set names	NES	NOM p-val
High-risk group	KEGG_STARCH_AND_SUCROSE_METABOLISM	1.47	0.048
Low-risk group	KEGG_MTOR_SIGNALING_PATHWAY	−1.70	0.008
	KEGG_TASTE_TRANSDUCTION	−1.67	0.004
	KEGG_GLYCOSAMINOGLYCAN_BIOSYNTHESIS_CHONDROITIN_SULFATE	−1.62	0.022
	KEGG_GLYCOSPHINGOLIPID_BIOSYNTHESIS_GANGLIO_SERIES	−1.60	0.026
	KEGG_GLYCEROPHOSPHOLIPID_METABOLISM	−1.58	0.012
	KEGG_ABC_TRANSPORTERS	−1.58	0.024
	KEGG_CALCIUM_SIGNALING_PATHWAY	−1.56	0.006
	KEGG_NEUROACTIVE_LIGAND_RECEPTOR_INTERACTION	−1.54	0.006
	KEGG_GNRH_SIGNALING_PATHWAY	−1.49	0.024
	KEGG_LONG_TERM_DEPRESSION	−1.45	0.045
	KEGG_MAPK_SIGNALING_PATHWAY	−1.43	0.050

4. Discussion

Tumors have complex metabolic changes known as metabolic reprogramming, which has been highlighted as a core marker of cancer [23]. Including catabolic and anabolic processes, metabolism participate in carcinogenic pathways and affect the growth and proliferation of cancer cells. Numerous targeted therapies and immunotherapies fail to show satisfying outcomes in PC [24, 25, 26], while the effect of reprogramming metabolism have been conducted on the occurrence and progression of PC [3]. Besides, the metabolism of PC is closely associated with chemo-resistance, radio-resistance, and immunosuppression [27, 28, 29]. However, PC can be divided into different metabolic subgroups, which predict different outcomes and responses to therapy [30]. Considering the rapid development of current high-throughput technology, the sequencing of potential genes or the whole genome can be utilized by specialized laboratories. This makes genomics research more closely linked to clinical diagnostic and therapeutic applications, allowing the data construction of gene-related prediction practical. Given the progression of PC, metabolic markers can predict patient response to individualized therapy. Characteristic changes in metabolic processes may occur more earlier than symptoms in the clinic. In view of few studies have focused on the prognostic characteristics of PC patients based on MRGs and IRGs. Here, we aimed to construct a comprehensive prognostic model to precisely predict the prognosis of PC patients from the above two aspects.

In this work, multiple bioinformatics analyses were carried out to construct a five-DEMRGs prognostic prediction model for PC. Furthermore, we also performed the western blotting experiment to validate all the five genes in model showed high protein expression in several PC cell lines. The PPI network indicated PTGS2 was the critical key gene. Upregulation of PTGS2 (also known as cyclooxygenase-2; COX-2) exerts its effect via the overproduction of prostaglandin E2 (PGE2). Therefore, the urinary PGE2 metabolites (PGE-M) may serve as a promising biomarker to predict PC risk [31]. As a COX-2 inhibitor, Celecoxib, together with Gemcitabine and Ironotecan, had been found to increase the overall survival of PC from about 6 months to 18 months [32]. And the mechanism of COX-2 has been shown to include effects on angiogenesis as well as apoptosis. It is crucial that the expression of COX-2 present during the early neoplastic changes of PC, well before progression to invasive disease. This indicates the five-DEMRGs that include COX-2 can make earlier clinical diagnosis of the disease [33]. The cBioPortal tool indicated that PIK3CA and IDO1 were the most commonly altered genes. The clinical data of PC downloaded from the TCGA database exhibited PIK3CA, ARG2 and PTGS2 were significantly correlated with age, histological grade, stage, and T classification (Supplementary *B). Furthermore, the above three genes were considered as oncogenes with HR $>$ 1 in this study. Regarded as a primary downstream target of the RAS family, PIK3CA involves in the regulation of proliferation and apoptosis in most cancers [34], and PIK3CA mutation had been reported in patients with carcinoma of pancreas [35]. Sivaram et al. demonstrated that tumor cell PIK3CA-AKT signaling could limit T cell recognition and clearance of PC cells [36]. By targeting PIK3CA to inhibit the phosphatidylinositol 3 kinase/AKT signaling pathway, miR-142-5p has been shown to inhibit pancreatic cancer migration and invasion [37]. In addition, a study displayed the PI3K/Akt/mTOR network signaling was activated in PC and the proliferation and drug resistance were regulated by this pathway. In IDO1 expressing tumors, tryptophan is a legitimate one-carbon source for the tetrahydrofoloc acid cycle. Also, IDO1 activity consumes tryptophan and the reduction of tryptophan decreases tumor-infiltrating T cell activity [38]. Interestingly, tryptophan is reported to be one of the most depleted interstitial nutrients in PC [39]. And a clinical trial had been proved the combination of navoximod (a IDO1 inhibitor) and atezolizumab demonstrated acceptable safety and tolerability for advanced cancer patients [40]. And in PC, the tumor suppressors ARG2 and PLCG1, show mRNA expression and protein levels that are significantly higher than in normal cells. ARG2 which is an extrahepatic mitochondrial enzyme, can catabolize arginine into ornithine and urea to induce obesity. The loss or silencing of ARG2 in human or mouse tumors strongly suppresses PDAC growth, especially in obese hosts [41]. However, a recent study indicates that ARG2 is expressed in lung cancer but it does not induce tumor immune escape and does not affect disease progression probably due to the lack of concomitant NOS expression [42]. By activating PLCG1, a novel member of the TSPAN superfamily-tetraspanin 1 may affect PC cell migration and invasion as well as MMP2 expression [43]. However, in myelodysplastic syndromes, reduced PLCG1 expression is associated with inferior survival [44]. We therefore speculate that the paradox of the opposing effects of ARG2 and PLCG1 expressions may be due to the specific environmental ways in which these two genes regulate cellular processes through different regulatory networks. Furthermore, from our study, the evidence of validation (ICGC-PAAD-US and GSE28735 datasets) and independent prognostic analyses further verified the feasibility of the prediction model, and risk scores from the model could act as independent

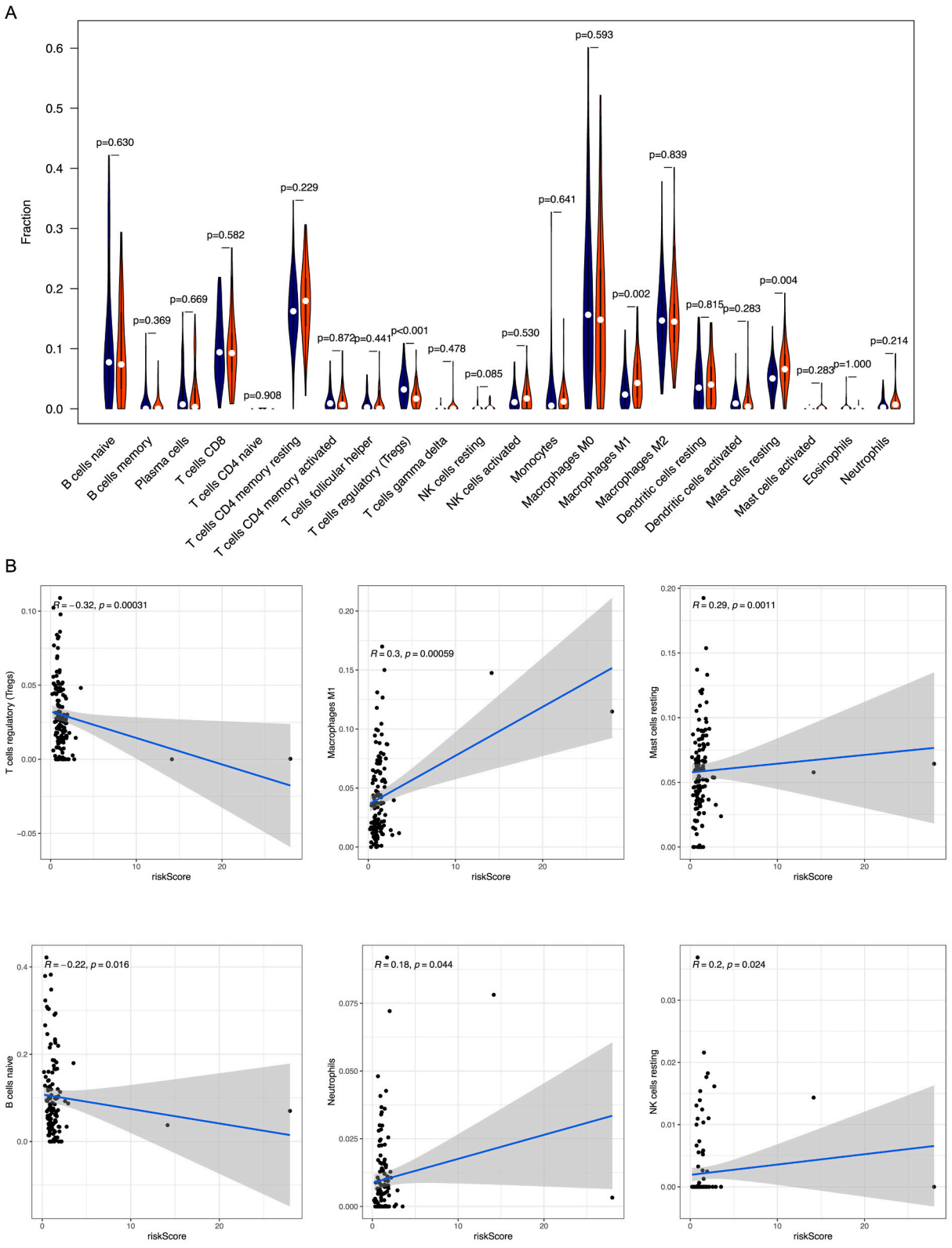

Figure 9. Difference and correlation analyses of tumor infiltrated immune cells. **(A)** Comparisons of 22 kinds of tumor infiltrated immune cells between high-risk and low-risk groups. The blue violin diagram presented low-risk group, and the red violin diagram on behalf of high-risk group. **(B)** The correlation between tumor infiltrated immune cells and the risk score.

Table 4
The intersection of difference analysis and correlation analysis.

Tumor infiltrated immune cells	Difference test (p-value)	Correlation test (*p*-value)
T-cells regulatory	<0.001	<0.001
Macrophages M1	0.002	<0.001
Mast cells resting	0.004	0.001

prognostic factors for PC. In addition, the AUC values at 2 or 3 years of the multivariate Cox regression analysis were more accurate when compared with the Lasso regression analysis, another commonly used bioinformatics model. The consequences of GSEA revealed that the high-risk group was enriched in starch and sucrose metabolism whilst the low-risk group was correlated with plentiful metabolic pathways, manifesting that an imbalance of the tumor metabolic microenvironment may affect the progression of PC.

Regulating the distribution and proportion of immune cells, tumor infiltrated immune cells are closely correlated with angiogenesis, metastasis, and proliferation of tumor cells. Tumor inflammation is extremely active, especially in the early stages of cancer [45]. In this study, we found the risk scores were associated with the early stages of PC, suggesting potential roles for risk scores in PC carcinogenesis. Infiltration of CD4+ CD25+ FOXP3+ Tregs is associated with immunologic tolerance and poor prognosis of PC [46]. Furthermore, circulating Tregs are regarded as prognostic factors for chemotherapeutic response in unresectable PC patients [47]. These phenomena demonstrate the vital role of Tregs in the PC tumor microenvironment. However, in this work, we discovered risk scores were negatively associated with Tregs. A previous study found that Tregs were dynamically distributed during tumorigenesis and progression. CD103+ was found to be recruited at day 7 but decreased with tumor progression [48]. Therefore, we speculated the association of risk scores and Tregs would be weakened during the development of PC. Acting as antitumor immune components, M1 macrophages have been shown to prevent immune escape in PC [49]. In early tumors, macrophages are mainly M1 type, which play pro-inflammatory tumoricidal roles [50]. Combined with the data from our study, we hypothesized that the correlation between M1 macrophages and risk scores may be an early event in PC carcinogenesis. Mast cells are the major component of the tumor immune microenvironment and regulate tumor progression by releasing pro-tumorigenic and anti-tumorigenic molecules [51]. Mediators such as IL-8, VEGF, and histamine are thought to promote tumor growth, while IL-1, IL-6 and TNF are thought to have anti-tumor growth properties. In our study, we found mast cell resting was greater in the high-risk group than the low-risk group, and risk scores were positively correlated with mast cell resting. Thus, these data further demonstrated that the association of risk scores and these immune cells is an early event in the progression of PC. Additionally, when exploring the correlation of the risk scores and ICGs, we found 12 differential expressed ICGs, indicating a potential relationship between the risk scores model and immunotherapy response. Most of these genes were overexpressed in the low-risk group, among which TNFRSF4 was one of the most significantly expressed genes. High expression of TNFRSF4 (also known as OX40) has been correlated with better overall survival colon cancer. In lymphomas, OX40 expression is significantly increased in CD4 T cells, and more specifically, OX40 expression can actually be used as a marker for tumor antigen-specific Tregs [52].

The five-DEMRGs model in this study proposed a new insight from tumor metabolism to predict PC prognosis when compared with previous studies. These five-DEMRGs were also immune genes, and these genes may achieve real-time detection of disease recurrence and treatment response after immune checkpoint inhibitor treatments and surgical resection. In addition, each of the five genes in this model has a close clinical correlation with PC. Screened by layers of bioinformatic analyses, this model can be more comprehensive, accurate and early to evaluate the prognosis and clinic of PC.

5. Conclusion

Collectively, our study identified and validated a five-DEMRGs model to independently predict PC prognosis. The prognostic significance of this model may contribute to monitor PC occurrence. Our study may also lead to individualized treatments, and provides new insights for PC prognosis.

Declarations

Author contribution statement

Huimin huang: Analyzed and interpreted the data; Wrote the paper. Shipeng Zhou; Xingling Zhao: Performed the experiments; Wrote the paper. Shitong Wang: Performed the experiments. Liyi Li; Linhua Lan; Huajun Yu: Conceived and designed the experiments; Wrote the paper.

Funding statement

Linhua Lan was supported by National Natural Science Foundation of China [81902803], Natural Science Foundation of Zhejiang Province [LY21H160057]. Dr. huimin huang was supported by Wenzhou Municipal Science and Technology Bureau [2021Y1012].

Data availability statement

Data associated with this study has been deposited the UCSC Xena database (https://xenabrowser.net/datapages/), the ImmPort database (http://www.immport.org/), the cBioPortal tool database (https://www.cbioportal.org), the ICGC database (https://icgc.org/) and the GEO database (https://www.ncbi.nlm.nih.gov/gds/).

Declaration of interest's statement

The authors declare no competing interests.

Additional information

Supplementary content related to this article has been published online at https://doi.org/10.1016/j.heliyon.2022.e12378.

References

[1] L. Rahib, B.D. Smith, R. Aizenberg, et al., Projecting cancer incidence and deaths to 2030: the unexpected burden of thyroid, liver, and pancreas cancers in the United States, Cancer Res. 74 (11) (2014) 2913–2921.
[2] L. Huang, L. Jansen, Y. Balavarca, et al., Resection of pancreatic cancer in Europe and USA: an international large-scale study highlighting large variations, Gut 68 (1) (2019) 130–139.
[3] C. Qin, G. Yang, J. Yang, et al., Metabolism of pancreatic cancer: paving the way to better anticancer strategies, Mol. Cancer 19 (1) (2020) 50.
[4] J. Chakladar, S.Z. Kuo, G. Castaneda, et al., The pancreatic Microbiome is associated with Carcinogenesis and worse prognosis in Males and Smokers, Cancers 12 (9) (2020).
[5] S.K. Kamarajah, W.R. Burns, T.L. Frankel, et al., Validation of the American Joint Commission on cancer (AJCC) 8th Edition staging system for patients with pancreatic adenocarcinoma: a Surveillance, Epidemiology and End results (SEER) analysis, Ann. Surg. Oncol. 24 (7) (2017) 2023–2030.
[6] M. Wu, X. Li, R. Liu, et al., Development and validation of a metastasis-related gene signature for predicting the overall survival in patients with pancreatic ductal adenocarcinoma, J. Cancer 11 (21) (2020) 6299–6318.
[7] D. Hanahan, R.A. Weinberg, Hallmarks of cancer: the next generation, Cell 144 (5) (2011) 646–674.
[8] R.A. Cairns, I.S. Harris, T.W. Mak, Regulation of cancer cell metabolism, Nat. Rev. Cancer 11 (2) (2011) 85–95.
[9] M.D. Hirschey, R.J. Deberardinis, A.M.E. Diehl, et al., Dysregulated metabolism contributes to oncogenesis, Semin. Cancer Biol. 35 (Suppl) (2015) S129–S150.
[10] O. Warburg, On the origin of cancer cells, Science 123 (3191) (1956) 309–314.
[11] O.G. Mcdonald, X. Li, T. Saunders, et al., Epigenomic reprogramming during pancreatic cancer progression links anabolic glucose metabolism to distant metastasis, Nat. Genet. 49 (3) (2017) 367–376.
[12] A. Carrer, S. Trefely, S. Zhao, et al., Acetyl-CoA metabolism supports multistep pancreatic tumorigenesis, Cancer Discov. 9 (3) (2019) 416–435.
[13] R.L. Chen, J.X. Zhou, Y. Cao, et al., Construction of a prognostic immune signature for squamous-cell lung cancer to predict survival, Front. Immunol. 11 (1933) (2020).
[14] C. Feig, A. Gopinathan, A. Neesse, et al., The pancreas cancer microenvironment, Clin. Cancer Res. 18 (16) (2012) 4266–4276.
[15] W. Zou, N.P.T.(H. Restifo, 17 cells in tumour immunity and immunotherapy, Nat. Rev. Immunol. 10 (4) (2010) 248–256.
[16] X. Li, M. Wenes, P. Romero, et al., Navigating metabolic pathways to enhance antitumour immunity and immunotherapy, Nat. Rev. Clin. Oncol. 16 (7) (2019) 425–441.
[17] J. Huo, L. Wu, Y. Zang, Development and validation of a novel metabolic-related signature predicting overall survival for pancreatic cancer, Front. Genet. 12 (2021), 561254.
[18] B. Liu, T. Fu, P. He, et al., Construction of a five-gene prognostic model based on immune-related genes for the prediction of survival in pancreatic cancer, Biosci. Rep. 41 (7) (2021).
[19] F.F. Hu, C.J. Liu, L.L. Liu, et al., Expression profile of immune checkpoint genes and their roles in predicting immunotherapy response, Briefings Bioinf. 22 (3) (2021).
[20] D.M. Pardoll, The blockade of immune checkpoints in cancer immunotherapy, Nat. Rev. Cancer 12 (4) (2012) 252–264.
[21] K.S. Campbell, A.K. Purdy, Structure/function of human killer cell immunoglobulin-like receptors: lessons from polymorphisms, evolution, crystal structures and mutations, Immunology 132 (3) (2011) 315–325.
[22] H. Afrache, P. Gouret, S. Ainouche, et al., The butyrophilin (BTN) gene family: from milk fat to the regulation of the immune response, Immunogenetics 64 (11) (2012) 781–794.
[23] L.K. Boroughs, R.J. Deberardinis, Metabolic pathways promoting cancer cell survival and growth, Nat. Cell Biol. 17 (4) (2015) 351–359.
[24] M. Feng, G. Xiong, Z. Cao, et al., PD-1/PD-L1 and immunotherapy for pancreatic cancer, Cancer Lett. 407 (2017) 57–65.
[25] M. Akce, M.Y. Zaidi, E.K. Waller, et al., The potential of CAR T cell therapy in pancreatic cancer, Front. Immunol. 9 (2166) (2018).
[26] C. Mosquera, D. Maglic, E.E. Zervos, Molecular targeted therapy for pancreatic adenocarcinoma: a review of completed and ongoing late phase clinical trials, Cancer Genet. 209 (12) (2016) 567–581.
[27] C. Grasso, G. Jansen, E. Giovannetti, Drug resistance in pancreatic cancer: Impact of altered energy metabolism, Crit. Rev. Oncol. Hematol. 114 (2017) 139–152.
[28] V. Gunda, J. Souchek, J. Abrego, et al., MUC1-Mediated metabolic alterations regulate response to Radiotherapy in pancreatic cancer, Clin. Cancer Res. 23 (19) (2017) 5881–5891.
[29] C.H. Chang, J. Qiu, D. O'sullivan, et al., Metabolic Competition in the tumor microenvironment is a Driver of cancer progression, Cell 162 (6) (2015) 1229–1241.
[30] K. Mehla, P.K. Singh, Metabolic Subtyping for novel personalized therapies against pancreatic cancer, Clin. Cancer Res. 26 (1) (2020) 6–8.
[31] Y. Cui, X.O. Shu, H.L. Li, et al., Prospective study of urinary prostaglandin E2 metabolite and pancreatic cancer risk, Int. J. Cancer 141 (12) (2017) 2423–2429.
[32] B.F. El-Rayes, M.M. Zalupski, A.F. Shields, et al., A phase II study of celecoxib, gemcitabine, and cisplatin in advanced pancreatic cancer, Invest. New Drugs 23 (6) (2005) 583–590.
[33] L.M. Knab, P.J. Grippo, D.J. Bentrem, Involvement of eicosanoids in the pathogenesis of pancreatic cancer: the roles of cyclooxygenase-2 and 5-lipoxygenase, World J. Gastroenterol. 20 (31) (2014) 10729–10739.
[34] M. Falasca, F. Selvaggi, R. Buus, et al., Targeting phosphoinositide 3-kinase pathways in pancreatic cancer-from molecular signalling to clinical trials, Anti Cancer Agents Med. Chem. 11 (5) (2011) 455–463.
[35] F. Schonleben, W. Qiu, H.E. Remotti, et al., PIK3CA, KRAS, and BRAF mutations in intraductal papillary mucinous neoplasm/carcinoma (IPMN/C) of the pancreas, Langenbeck's Arch. Surg. 393 (3) (2008) 289–296.

[36] N. Sivaram, P.A. Mclaughlin, H.V. Han, et al., Tumor-intrinsic PIK3CA represses tumor immunogenecity in a model of pancreatic cancer, J. Clin. Invest. 129 (8) (2019) 3264–3276.
[37] J. Zhu, L. Zhou, B. Wei, et al., miR1425p inhibits pancreatic cancer cell migration and invasion by targeting PIK3CA, Mol. Med. Rep. 22 (3) (2020) 2085–2092.
[38] D.H. Munn, M.D. Sharma, B. Baban, et al., GCN2 kinase in T cells mediates proliferative arrest and anergy induction in response to indoleamine 2,3-dioxygenase, Immunity 22 (5) (2005) 633–642.
[39] A.C. Newman, M. Falcone, A. Huerta Uribe, et al., Immune-regulated Ido1-dependent tryptophan metabolism is source of one-carbon units for pancreatic cancer and stellate cells, Mol. Cell 81 (11) (2021) 2290–22302 e7.
[40] K.H. Jung, P. Lorusso, H. Burris, et al., Phase I study of the indoleamine 2,3-dioxygenase 1 (Ido1) inhibitor navoximod (GDC-0919) Administered with PD-L1 inhibitor (atezolizumab) in advanced Solid tumors, Clin. Cancer Res. 25 (11) (2019) 3220–3228.
[41] T. Zaytouni, P.Y. Tsai, D.S. Hitchcock, et al., Critical role for arginase 2 in obesity-associated pancreatic cancer, Nat. Commun. 8 (1) (2017) 242.
[42] R. Rotondo, L. Mastracci, T. Piazza, et al., Arginase 2 is expressed by human lung cancer, but it neither induces immune suppression, nor affects disease progression, Int. J. Cancer 123 (5) (2008) 1108–1116.
[43] Zhang Gang Xiaobo, et al., TSPAN1 upregulates MMP2 to promote pancreatic cancer cell migration and invasion via PLCγ, Oncol. Rep. 41 (4) (2019) 2117–2125.
[44] M. Shiseki, M. Ishii, M. Miyazaki, et al., Reduced PLCG1 expression is associated with inferior survival for myelodysplastic syndromes, Cancer Med. 9 (2) (2020) 460–468.
[45] P. Neviani, P.M. Wise, M. Murtadha, et al., Natural killer-Derived Exosomal miR-186 inhibits Neuroblastoma growth and immune escape mechanisms, Cancer Res. 79 (6) (2019) 1151–1164.
[46] T. Yamamoto, H. Yanagimoto, S. Satoi, et al., Circulating CD4+CD25+ regulatory T cells in patients with pancreatic cancer, Pancreas 41 (3) (2012) 409–415.
[47] C. Liu, H. Cheng, G. Luo, et al., Circulating regulatory T cell subsets predict overall survival of patients with unresectable pancreatic cancer, Int. J. Oncol. 51 (2) (2017) 686–694.
[48] B.M. Allen, K.J. Hiam, C.E. Burnett, et al., Systemic dysfunction and plasticity of the immune macroenvironment in cancer models, Nat. Med. 26 (7) (2020) 1125–1134.
[49] K. Young, R.T. Lawlor, C. Ragulan, et al., Immune landscape, evolution, hypoxia-mediated viral mimicry pathways and therapeutic potential in molecular subtypes of pancreatic neuroendocrine tumours, Gut 70 (10) (2021) 1904–1913.
[50] D.I. Gabrilovich, S. Ostrand-Rosenberg, V. Bronte, Coordinated regulation of myeloid cells by tumours, Nat. Rev. Immunol. 12 (4) (2012) 253–268.
[51] G. Varricchi, M.R. Galdiero, S. Loffredo, et al., Are mast cells MASTers in cancer? Front. Immunol. 8 (2017) 424.
[52] S. Aspeslagh, S. Postel-Vinay, S. Rusakiewicz, et al., Rationale for anti-OX40 cancer immunotherapy, Eur. J. Cancer 52 (2016) 50–66.